

Grid Connected System for Two-stage Solar Photovoltaic Based Stand-Alone Scheme Having Battery as energy storage

G.S.S.V.PRASAD

M-tech Student Scholar

Department of Electrical & Electronics Engineering,
Gonna Institute of Information Technology & Sciences
Visakhapatnam (Dt); A.P, India.
E-mail:sivag2400@gmail.com

P.LAVANYA

Assistant Professor

Department of Electrical & Electronics Engineering,
Gonna Institute of Information Technology & Sciences;
Visakhapatnam (Dt); A.P, India.
E-mail:plavanya38@gmail.com

Abstract—Stand alone renewable energy based on photovoltaic systems accompanied with battery storage system are beginning to play an important role over the world to supply power to remote areas. The objective of the study reported in this paper is to elaborate and design a bond graphs model for sizing standalone domestic solar photovoltaic electricity systems and simulating the performance of the systems in a tropical climate. The systems modelled consist of an array of PV modules, a lead-acid battery, and a number of direct current appliances. This paper proposes the combination of lead acid battery system with a typical stand alone photovoltaic energy system under variable loads. The main activities of this work purpose to establish library graphical models for each individual component of standalone photovoltaic system. With solar customers in many states now receiving a low price for electricity sold back to the grid, battery back-up systems can be a viable alternative as they use the electricity stored during the day to run your house at night. They also have the advantage of being able to supply power during power outages. Grid-connected systems do not need batteries which reduces considerably initial capital costs and energy costs. For a comparable load, grid-tied systems use smaller PV arrays than stand-alone systems. In order to address this issue, a two-stage stand-alone scheme consisting of a novel transformer coupled dual-input converter (TCDIC) followed by a conventional full-bridge inverter is proposed. The proposed TCDIC can realize maximum power point tracking and battery charge control while maintaining the proper voltage level at the load terminal. A suitable control strategy for the proposed TCDIC devised for manipulating the TCDIC to realize the first two aforementioned objectives, while the third objective is achieved by employing a conventional proportional integral (PI) controller to control the output voltage of the full bridge inverter through sinusoidal pulse width modulation. The simulation results are performed by using Matlab/Simulink software.

1. INTRODUCTION

Renewable energy sources (solar, wind, etc) are attracting more attention as alternative energy sources than conventional fossil fuel energy sources. This is not only due to the diminishing fuel sources, but also due to environmental pollution and global warming problems. Among these sources is the solar energy, which is the

most promising, as the fabrication of less costly photovoltaic (PV) devices becomes a reality [1]. With increased penetration of solar PV devices, various antipollution apparatus can be operated such as water purification through electrochemical processing and stopping desert expansion by PV water pumping with tree plantation. However, control problems arise due to large variances of PV output power under different insolation levels. Solar energy is attractive, because it directly converts solar radiation energy in to electricity [2]. Its energy conversion and control system are simple and easy to maintain. Being inherently sustainable and eco-friendly, the PV based systems are gaining popularity [3]. Photovoltaic applications can be broadly classified into two categories. One is the standalone system and other is the grid connected system. The standalone system is widely used in remote places where access to electricity is not viable. The standalone configuration can provide a well regulated load voltage but the reliability of power supply cannot be guaranteed [4]. Storage batteries are widely used to improve their liability of the standalone system [5]. The integration of PV system to the grid is rapidly increasing due to the improvement in the power electronics technology. Generally, single phase or three phase voltage source inverters (VSI) are used for interfacing PV system to grid and employs a controller to stabilize the DC bus voltage and regulate the current injected into the grid. Various topologies and control strategies for grid connected inverters have been reported in literature. The grid connected PV systems (GCPV), feeding active power to the grid can be controlled to supply there active power demand of the load [6-8].

High-gain multi winding transformer-based converters can be used to address this issue. However, such systems require a minimum of eight controlled switches. This is in addition to the four switches that are required to realize the inverter. Furthermore, existing stand-alone schemes employ an additional dedicated dc-dc converter to realize MPP operation. As PV power remains unavailable for more than half of a day, the utilization of this

aforementioned dedicated converter becomes very poor [9].

A scheme wherein the use of a dedicated dc–dc converter for MPPT operation is avoided is proposed. This scheme has the PV array and battery connected in series and is designed for application in PV-powered lighting system. However, the scheme presented has the following limitations:

- 1) The presence of resonant elements makes the system sensitive to parameter variation;
- 2) Permissible variation in the duty ratio of the switches is limited within a certain range; and
- 3) Voltage gain is quite limited. A similar approach has also been reported for application in a grid-connected scheme.

However, the aforementioned schemes have to bypass the PV array by a diode and an inductor when PV power goes to zero.

This results in overall gain reduction as the PV and battery are connected in series.

In order to address the limitations encountered, a transformer-coupled dual-input converter (TCDIC)-based stand-alone scheme is proposed in this paper. The input stage of the proposed TCDIC is realized by connecting the PV array in series with the battery, thereby facilitating the boosting capability of the converter. The output voltage level of the TCDIC is further enhanced by incorporating a high-frequency step-up transformer. The unique feature of TCDIC is that it can be made to perform MPPT operation, battery charge control, and voltage boosting by employing a proper control algorithm [10].

Hence, all of the facilities that are achieved in the existing stand-alone schemes by involving two or more stages of dc–dc converters can be obtained by employing the proposed single stage TCDIC. A standard full-bridge inverter is employed at the output of TCDIC to achieve dc–ac conversion. The basic philosophy of this scheme and its very preliminary study have been presented, and subsequently, further work that has been carried out on this scheme is presented in this paper [11].

A photovoltaic (PV) system is able to supply electric energy to a given load by directly converting solar energy through the photovoltaic effect. The system structure is very flexible. PV modules are the main building blocks; these can be arranged into arrays to increase electric energy production. Normally additional equipment is necessary in order to transform energy into a useful form or store energy for future use. The resulting system will therefore be determined by the energy needs (or loads) in a particular application. PV systems can be broadly classified in two major groups [12]

1) Grid-Tied: These systems are directly coupled to the electric distribution network and do not require battery storage. Figure.1 describes the basic system configuration. Electric energy is either sold or bought from the local electric utility depending on the local

energy load patterns and the solar resource variation during the day, this operation mode requires an inverter to convert DC currents to AC currents. There are many benefits that could be obtained from using grid-tied PV systems instead of the traditional stand-alone schemes. These benefits are:

- Smaller PV arrays can supply the same load reliably.
- Less balance of system components are needed.
- Comparable emission reduction potential taking advantage of existing infrastructure.
- Eliminates the need for energy storage and the costs associated to substituting and recycling batteries for individual clients. Storage can be included if desired to enhance reliability for the client.
- Takes advantage of the existing electrical infrastructure.
- Efficient use of available energy. Contributes to the required electrical grid generation while the client's demand is below PV output.

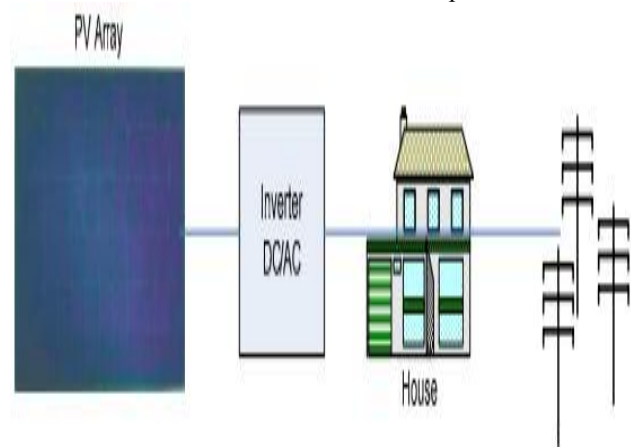


Fig.1.Grid-Tied Photovoltaic System.

Hybrid systems may be possible were battery storage or a generator (or both) can be combined with a grid connection for additional reliability and scheduling flexibility (at additional cost). [13] Most of the installed residential, commercial and central scale systems use pre-fabricated flat plate solar modules, because they are widely available. Most 5-7 available reports on PV system costs are therefore related to this kind of technology and shall be our focus in this chapter. Other specialized technologies are available (e.g., concentrating PV systems), but not as commercially available as the traditional PV module.

II. OPERATING PRINCIPLE OF TCDIC

The schematic diagram of the TCDIC is depicted in Fig. 2. From this figure, it can be noted that no dedicated converter

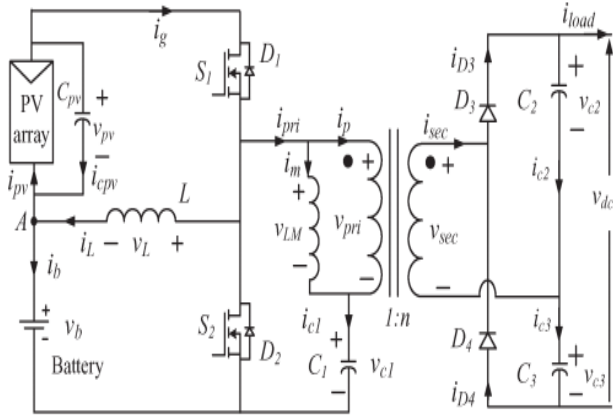


Fig. 2. Schematic circuit diagram of TCDIC.

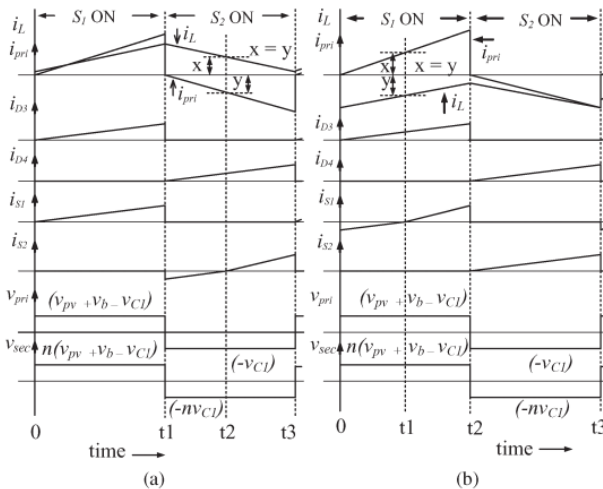


Fig. 3. Waveforms of currents flowing through and voltage across different key circuit elements of TCDIC when (a) i_L is positive and (b) i_L is negative.

is employed for ensuring the MPP operation of the PV array, which leads to the improved utilization of the converters involved. Furthermore, only one converter stage is present in the path between the PV array and the battery, thereby improving the charging efficiency of the battery. The inductor current i_L is designed to be continuous. The switches S_1 and S_2 are operated in complementary fashion. All semiconductor devices and passive elements are assumed to be ideal in the following analysis.

A. Operation of the Converter When Inductor Current is Positive

The waveforms of the currents flowing through and voltages across different key circuit elements of TCDIC, while the current flowing through the inductor L is positive, are shown in Fig. 3(a). The various possible switching modes during this condition are analyzed in this section.

a) Mode I (0 to t_1 ; S_1 and D_3 conducting): When S_1 is turned on, the PV array voltage v_{pv} is impressed across L , and the inductor current i_L increases. During this period, the voltage impressed across the primary winding of the transformer is $v_{pri} = (v_{pv} + v_b - v_{C1})$, wherein v_b is the

battery voltage and v_{C1} is the voltage across the capacitor C_1 . Hence, the primary current of the transformer, i_{pri} , increases, and the capacitor C_1 gets charged. The current flowing through the secondary

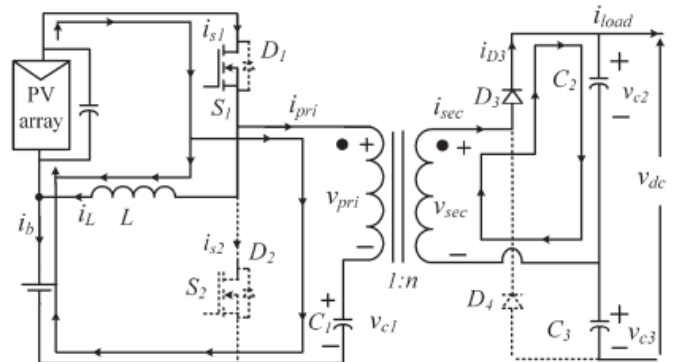


Fig. 4. Equivalent circuit diagram of TCDIC when operating in mode I and inductor current is positive.

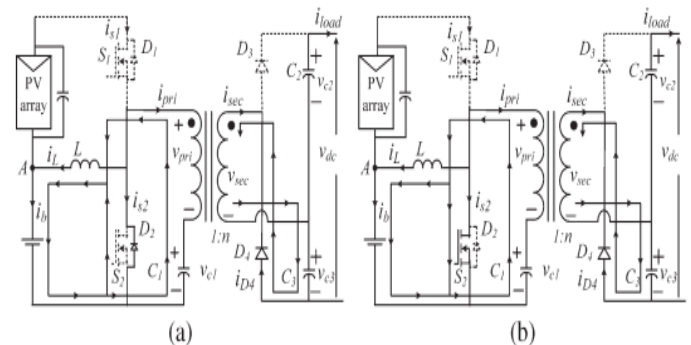


Fig. 5. Equivalent circuit diagram of TCDIC when inductor current is positive: (a) Mode II and (b) mode III.

Winding of the transformer, i_{sec} , also increases. The diode D_3 is forward biased, and the capacitor C_2 gets charged. The voltage across C_2 is given by $v_{C2} = n(v_{pv} + v_b - v_{C1})$, wherein n is the turns ratio of the transformer. The equivalent diagram of TCDIC during this mode is shown in Fig. 4.

b) Mode II (t_1 to t_2 ; D_2 and D_4 conducting): This mode begins when S_1 is turned off and S_2 is turned on. At the starting of this mode, i_L is positive, and as S_1 is turned off, i_{pri} is zero. Since $i_L > i_{pri}$, the diode D_2 starts conducting.

The voltage impressed across L is $v_L = -v_b$, and hence, i_L starts decreasing. The voltage impressed across the primary winding of the transformer is $v_{pri} = -v_{C1}$, and hence, i_{pri} becomes negative and starts decreasing, thereby discharging C_1 . The current flowing through the secondary winding of the transformer, i_{sec} , reverses, and the diode D_4 gets turned on. The capacitor C_3 is getting charged, and the voltage across C_3 can be expressed as $v_{C3} = n(v_{C1})$. During this mode, $i_L > (-i_{pri})$ and diode D_2 is forward biased. This mode continues until i_L becomes equal to $(-i_{pri})$. The equivalent circuit diagram of TCDIC during this mode is shown in Fig. 6(a).

c) Mode III (t₂ to t₃; S₂ and D₄ conducting): When i_L becomes smaller than $(-ipri)$, the diode D₂ is reverse biased, and the switch S₂ starts conducting. The rest of the operation remains the same as that of mode II. The equivalent circuit diagram of TCDIC during this mode is shown in Fig. 5(b).

B. Operation of the Converter When Inductor Current is Negative

The waveforms of the currents flowing through and voltages across different key circuit elements of TCDIC, while the current flowing through the inductor L is negative, are shown in Fig. 5(b). The various possible switching modes during this condition are analyzed in this section.

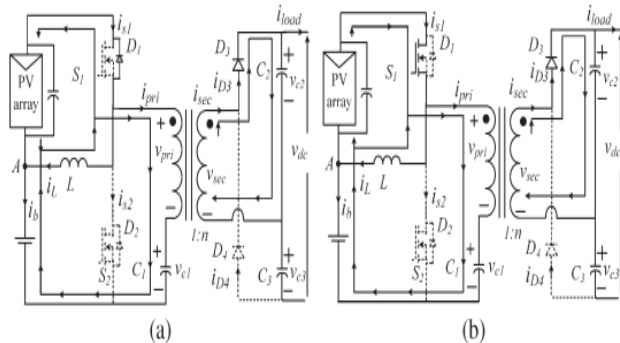


Fig. 6. Equivalent circuit diagram of TCDIC when inductor current is negative: (a) Mode I and (b) mode II.

d) Mode I (0 to t₁; D₁ and D₃ conducting): This mode begins when S₁ is turned on and S₂ is turned off. At the starting of this mode, i_L is negative, and $ipri$ is zero. Hence, the diode D₁ starts conducting. The rest of the operation is the same as that of mode I discussed in the previous section. This mode continues until $ipri$ becomes equal to $(-i_L)$. The equivalent circuit diagram of TCDIC during this mode is shown in Fig. 6(a).

e) Mode II (t₁ to t₂; S₁ and D₃ conducting): When $ipri$ becomes greater than $-i_L$, the diode D₁ is reverse biased, and the switch S₁ starts conducting. The rest of the operation is the same as that of mode I discussed in the previous section. The equivalent circuit diagram of TCDIC during this mode is shown in Fig. 6(b).

f) Mode III (t₂ to t₃; S₂ and D₄ conducting): This mode begins when S₁ is turned off and S₂ is turned on. During this mode, both i_L and $ipri$ are negative, and the switch S₂ conducts. The negative current in the primary winding of the transformer results in negative current in the secondary winding of the transformer. Hence, the diode D₄ is forward biased, and the capacitor C₃ gets charged. During operation in this mode, $v_L = -v_b$, $v_{pri} = -v_{C1}$, and $v_{C3} = nV_{C1}$. The equivalent circuit diagram of TCDIC during this mode is the same as that shown in Fig. 6(b), except that the direction of i_L is reversed. From Fig. 2, the voltage v_L across the inductor L can be expressed as

$$\begin{aligned} v_L &= v_{pv}, & \text{when } S_1 \text{ is on} \\ v_L &= -v_b, & \text{when } S_2 \text{ is on} \end{aligned} \quad (1)$$

Therefore, the average voltage drop across the inductor is

$$V_L = DV_{pv} - (1 - D)V_b$$

Wherein D is the duty ratio of the switch S₁. Equating the average voltage drop across the inductor to zero,

$$V_{pv} = \left[\frac{(1 - D)}{D} \right] V_b \quad (2)$$

From (2), it can be inferred that the PV voltage can be controlled by manipulating D as battery voltage V_b can be assumed to be a stiff source. Therefore, the MPPT operation of the PV array can be achieved through a proper manipulation of D. The average output voltage of the TCDIC, V_{dc} , is given by

$$\begin{aligned} V_{dc} &= (V_{C2} + V_{C3}) \\ &= [n(V_b + V_{pv} - V_{C1}) + nV_{C1}] \\ &= n(V_b + V_{pv}). \end{aligned} \quad (3)$$

Applying KCL at point A of Fig. 2,

$$i_L + i_{cpv} = i_b + i_{pv} \quad (4)$$

Considering the average values of i_L , i_{cpv} , i_b , and i_{pv} over a switching cycle and noting that $\bar{i}_{cpv} = 0$, (4) transforms to

$$I_b = I_L - I_{pv} \quad (5)$$

From (5), it can be noted that, for $I_L > I_{pv}$, the battery is charged and, for $I_L < I_{pv}$, the battery is discharged. Therefore, by controlling I_L , for a given I_{pv} , battery charging and discharging can be controlled. The drawback of TCDIC and the associated design constraints are presented. The details of the control strategy devised for TCDIC are discussed.

IV. CONTROL STRUCTURE

The controller of a stand-alone system is required to perform the following tasks: 1) extraction of maximum power from the PV array; 2) manipulate the battery usage without violating the limits of overcharge and overdischarge; and 3) dc-ac conversion while maintaining the load voltage at the prescribed level. A controller is devised for manipulating the TCDIC to realize the first two aforementioned objectives, while the third objective is achieved by employing a conventional proportional integral (PI) controller to control the output voltage of the fullbridge inverter through sinusoidal pulse width modulation. As the conventional control scheme is used for controlling the output voltage of the inverter, its design issues are not discussed in this paper. The details

of the control algorithm devised for TCDIC are presented in this section. In order to achieve the desired functionalities, TCDIC is required to operate in one of the following modes.

1) MPPT mode: Maximum power is extracted from the PV array when the system is operating in this mode. However, in order to operate in this mode, one of the following conditions must be satisfied: 1) Available maximum PV power P_{mpp} is more than the load demand P_l , and the surplus power can be consumed by the battery without being overcharged; and 2) $P_{mpp} < P_l$ and the battery have the capability to supply $P_l - P_{mpp}$ without being overdischarged. The PV power in MPPT mode is given by $P_{pv} = P_{mpp} = (P_b + P_l)$, where P_b is the battery power which is defined as positive during charging and negative while discharging.

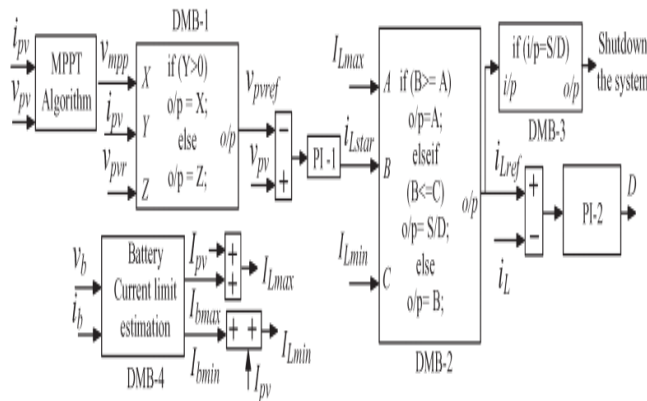


Fig. 8. Control structure for the proposed TCDIC.

2) Non-MPPT mode: Based on the state of charge (SOC) level of the battery, its charging current is required to be limited to a maximum permissible limit $I_{b \max}$ to prevent the battery from getting damaged due to overcharge. The maximum charging current limit $I_{b \max}$ restricts the maximum power that can be absorbed by the battery to $P_{b \max} = I_{b \max} * V_b$. When $P_{mpp} > P_l$ and the surplus power is more than $P_{b \max}$, the system cannot be operated in MPPT mode as it would overcharge the battery. During this condition, power extraction from PV is reduced to a value given by $P_{pv} = (P_{b \max} + P_l)$. This mode of operation is known as non-MPPT mode.

3) Battery only (BO) mode: The system operates in BO mode when there is no PV power and the battery has the capability to supply the load demand without being overdischarged.

4) Shutdown mode: When $P_{mpp} < P_l$ and the battery does not have the capability to supply $P_l - P_{mpp}$, the system needs to be shut down to prevent the battery from being overdischarged.

The control algorithm that is employed to select the proper mode of operation for the TCDIC, depending on the status of the SOC of the battery vis-a-vis the availability of power from the solar array, is shown in Fig.8. The proper mode selection is done by four logical decision-making blocks (DMBs). The control block

DMB-1 sets the reference for the PV array voltage (V_{pvref}). It also decides whether the system will operate in BO mode or in MPPT mode. When it is found that $i_{pv} > 0$, thereby indicating the availability of PV power, the MPPT mode of operation is selected, and the output of the MPPT algorithm block (i.e., V_{mpp}) sets V_{pvref} . When the PV power is not available, the BO mode is selected, and V_{pvref} is taken as V_{pvr} wherein V_{pvr} is selected so as to maintain the output voltage V_{dc} within the desired range of 350–460 V as per (3). The error between V_{pvref} and V_p is passed through a PI controller to set the required reference for the inductor current (i_{Lstar}). An upper limit $I_{L \max}$ and a lower limit $I_{L \min}$ is imposed on i_{Lstar} based on the relationship given in (5) to prevent overcharging and overdischarging of the battery, respectively. These two limits are derived as follows:

$$I_{L \max} = I_{b \max} + I_{pv}$$

$$I_{L \min} = I_{b \min} + I_{pv}$$

Wherein $I_{b \max}$ and $I_{b \min}$ are the maximum permissible charging and discharging current of the battery, respectively. These two limits are set based on the SOC level and the allowable depth of discharge of the battery. The block DMB-4 is employed to carry out the aforementioned functions. The block DMB-2 sets the reference level for the inductor current i_{Lref} after resolving the constraints imposed by $I_{L \max}$ and $I_{L \min}$.

When i_{Lref} remains within its prescribed limit, the system operates either in MPPT mode (for $i_{pv} > 0$) or in BO mode (for $i_{pv} \leq 0$). When i_{Lref} hits its lower limit, thereby indicating that the overdischarge limit of the battery is reached, DMB-3 withdraws gating pulses from all the switches and shuts down the system. When the battery overcharging limit is attained, i_{Lref} hits its upper limit. This situation arises only when the system is operating in MPPT mode with $P_{mpp} > P_l$ and the surplus power is more than $P_{b \max}$. In this condition, i_{Lref} is limited to $I_{L \max}$ to limit the battery charging current to $I_{b \max}$, and the MPPT is bypassed. As the battery charging current is limited to $I_{b \max}$, power consumed by the battery is restricted to $P_{b \max}$. This makes the available PV power more than $(P_l + P_{b \max})$. This extra PV power starts charging the PV capacitor, and its voltage increases beyond V_{mpp} , thereby shifting the PV operating point toward the right side of the MPP point, and the power extracted from the PV array reduces. This process continues until the power drawn from the PV array becomes equal to $(P_l + P_{b \max})$. Hence, during operation of the system in non-MPPT mode, the PV array is operated at a point on the right side of its true MPP, and hence, $P_{pv} < P_{mpp}$. If there is a decrement in load demand while operating in non-MPPT mode, power drawn from the PV array becomes more than $(P_l + P_{b \max})$, and this excess power drawn starts charging the PV capacitor, thereby shifting the operating point of the PV further toward the right side of its previous operating

point. In case of an increment in the load demand, the power drawn from the PV array falls short of supplying the load demand and the dc-link capacitors, and the PV capacitor starts discharging. As the voltage of the PV capacitor falls, the operating point of the PV array shifts toward the left side from its previous operating point. This leads to an increment in the power drawn from the PV array, and this process continues until the power balance is restored. In case the load demand increases to an extent such that the PV power available at its MPP falls short to supply this load, the battery will come out of its charging mode, iL_{ref} will become less than I_{Lmax} , and the system operates in MPPT mode.

V.MATLAB/SIMULATION RESULTS

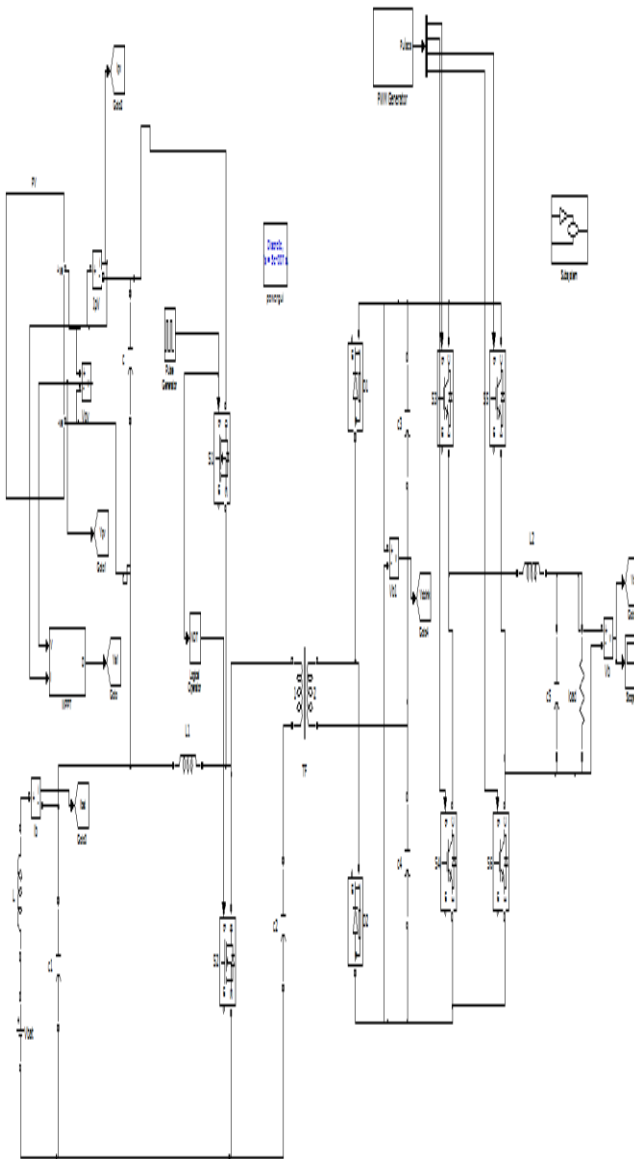


Fig.9. Matlab/Simulation model of under steady-state operation.

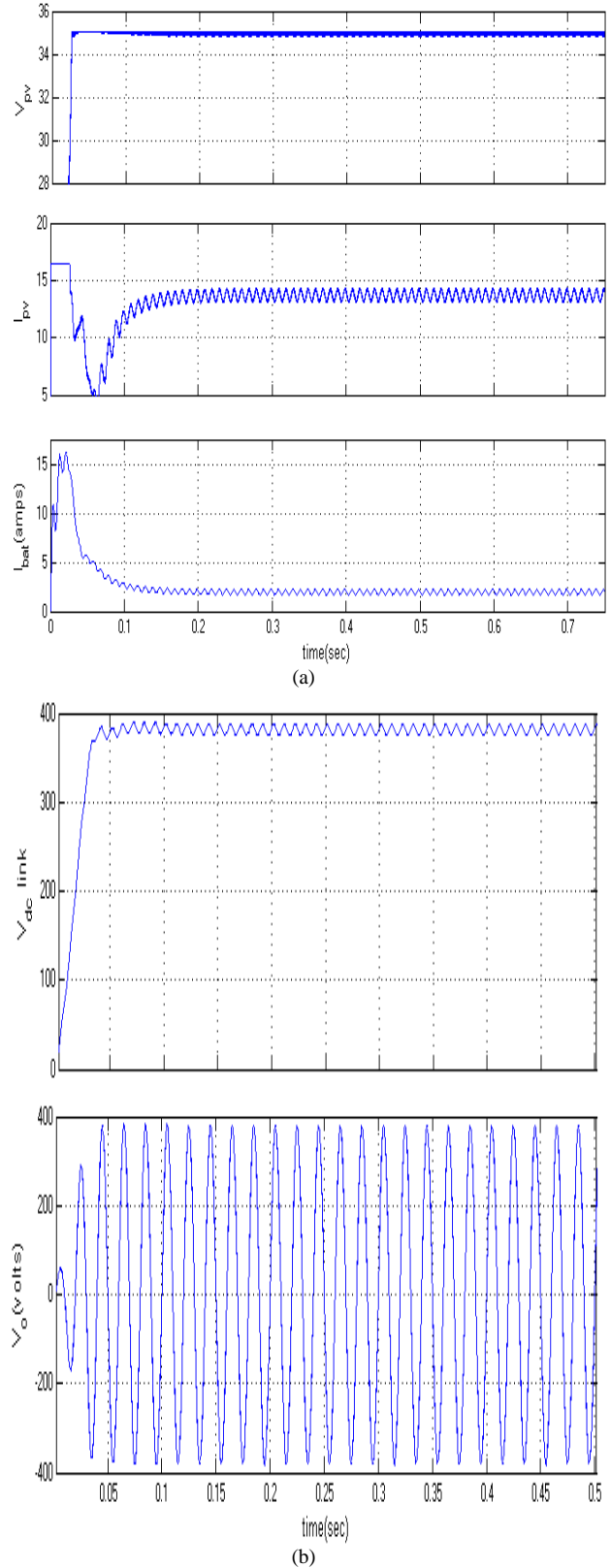


Fig. 10. Simulated response of the system under steady-state operation in MPPT mode. (a) vpv, ipv, and ib. (b) vdc and load voltage.

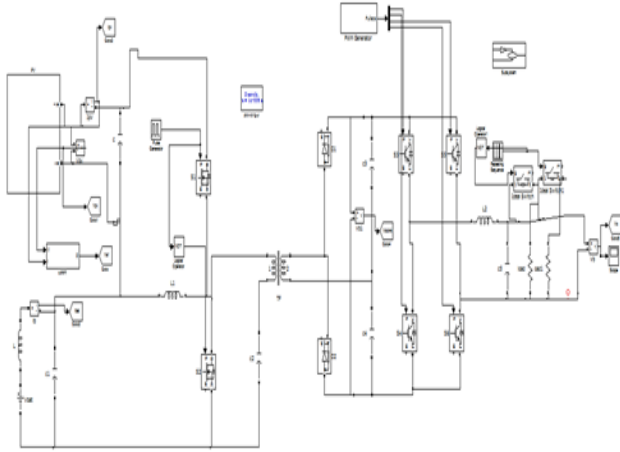
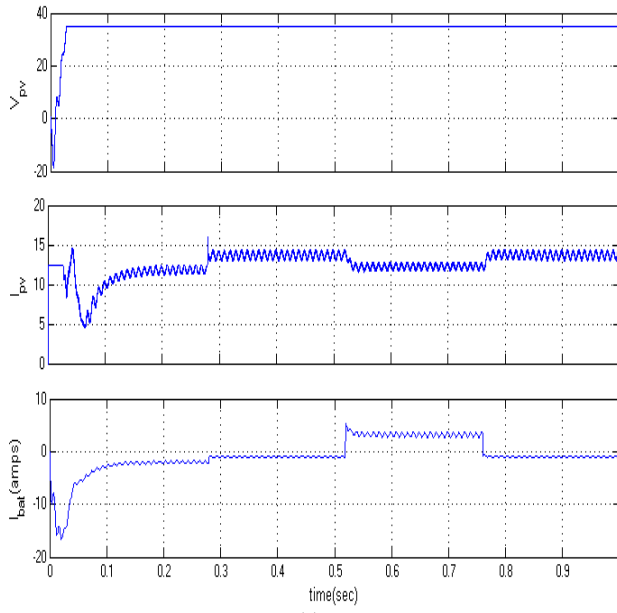
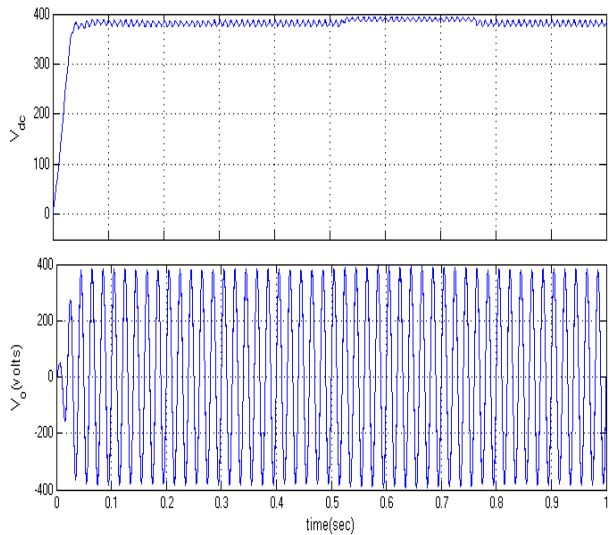


Fig.11. Matlab/Simulation model of under changes in load and insolation level while operating in MPPT mode.



(a)



(b)

Fig. 12. Simulated response of the system under changes in load and insolation level while operating in MPPT mode. (a) v_{pv} , i_{pv} , and i_b . (b) v_{dc} and load voltage.

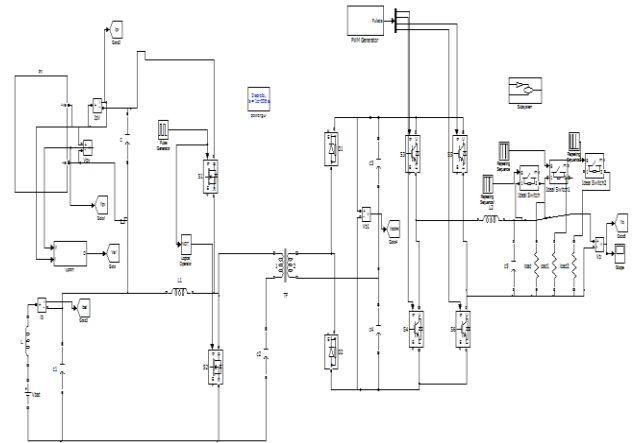
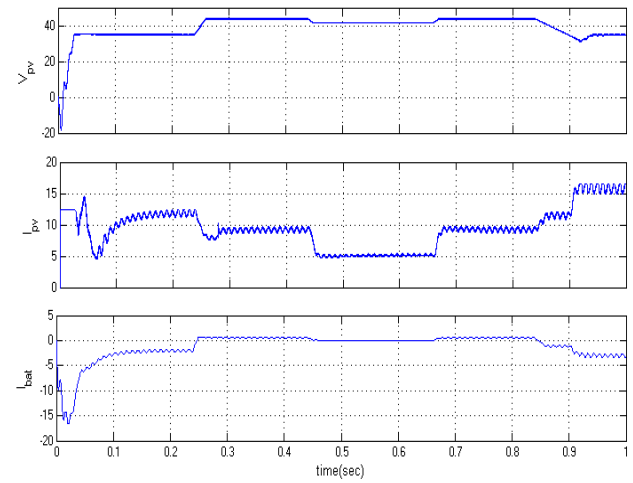
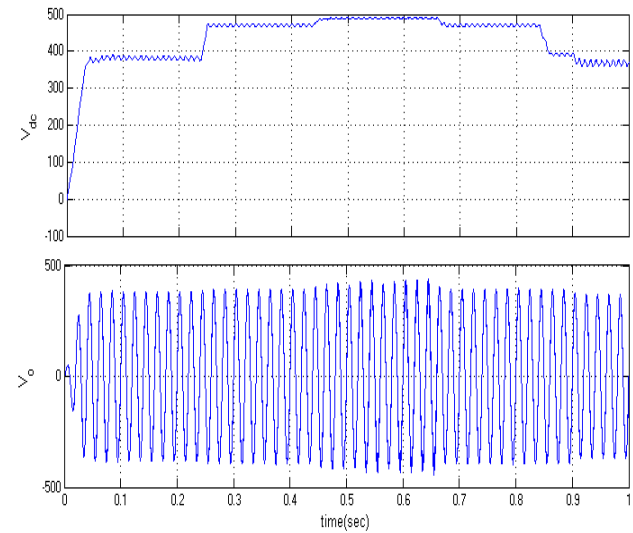


Fig.13. Matlab/Simulation model of under mode transition between MPPT and non MPPT mode and the effect of load change in non-MPPT mode.



(a)



(b)

Fig. 14. Simulated response of the system under mode transition between MPPT and non-MPPT mode and the effect of load change in non-MPPT mode. (a) v_{pv} , i_{pv} , and i_b . (b) v_{dc} and load voltage.

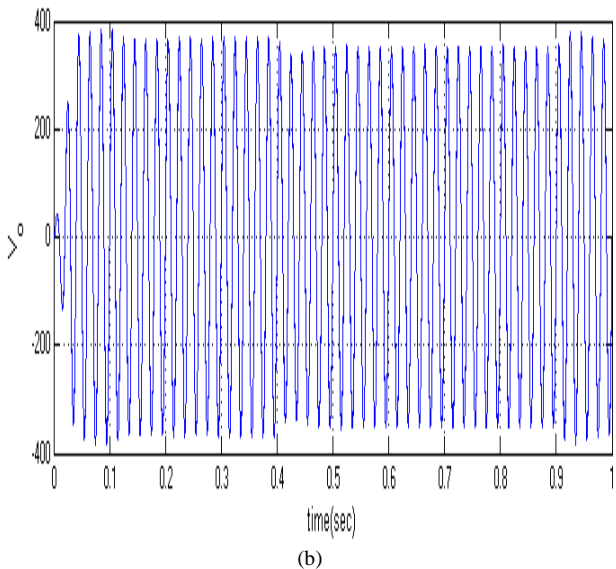
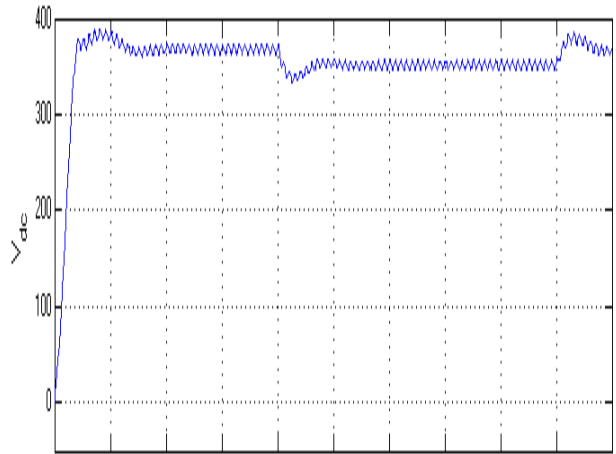
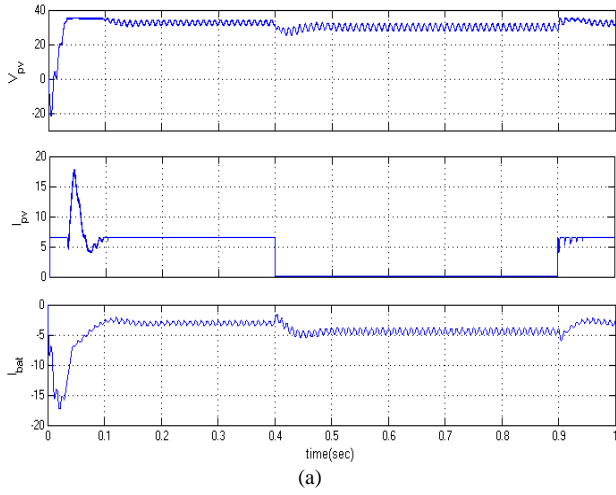


Fig. 15. Response of the simulated system during mode transition between MPPT and BO modes. (a) v_{pv} , i_{pv} , and i_b . (b) v_{dc} and load voltage.

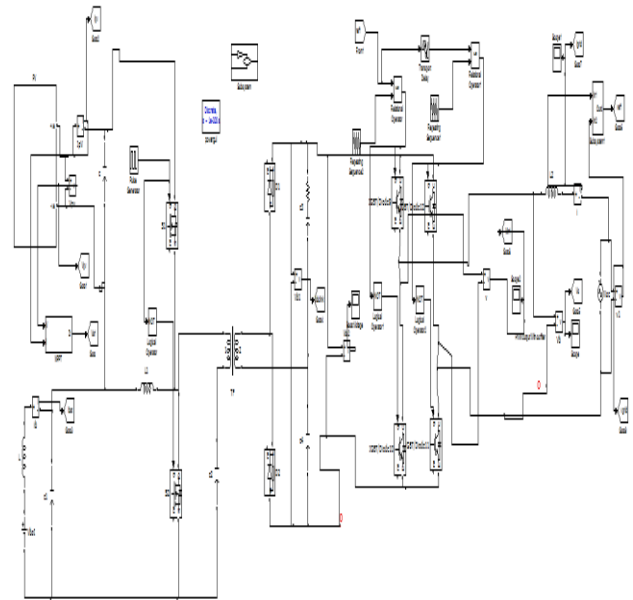


Fig.16. Matlab/Simulation model of under grid connected system.

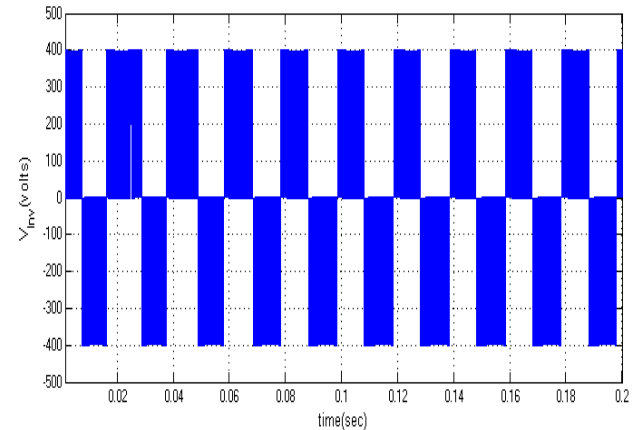


Fig.17. Inverter Output Voltage.

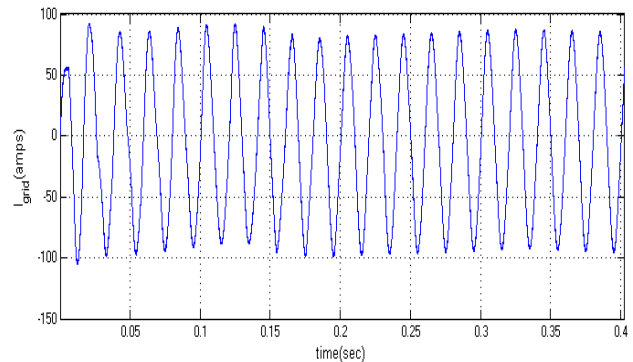


Fig.18. Grid Current.

VI. CONCLUSION

Solar PV is used primarily for grid-connected electricity to operate residential appliances, commercial equipment, lighting and air conditioning for all types of buildings. Through stand-alone systems and the use of batteries, it is also well suited for remote regions where there is no

electricity source. Solar PV panels can be ground mounted, installed on building rooftops or designed into building materials at the point of manufacturing. Performances of the management in real conditions strongly depend of the accuracy of the forecasts and of the mode of operation. This important conclusion leads to many questions about reactive power management without denying the importance and the necessity of the predictive optimization stage. The management developed helps integration of PV power into the grid as peak loads are shaved. Depending of the reactive management in real conditions, the power fluctuation of the PV production is balanced to the power exchanged with the grid or with the batteries. In this context, next and future works will deal with reactive management for real condition operations. The management developed helps integration of PV power into the grid as peak loads are shaved. Depending of the reactive management in real conditions, the power fluctuation of the PV production is balanced to the power exchanged with the grid or with the batteries.

REFERENCES

- [1]. Hamid R. Teymour, Danny Sutanto, Kashem M. Muttaqi, and P. Ciufo, —Solar PV and Battery Storage Integration using a New Configuration of a Three-Level NPC Inverter With Advanced Control Strategy IIEEE transactions on energy conversion, vol. 29, no. 2, June, 2014.
- [2]. O. M. Toledo, D. O. Filho, and A. S. A. C. Diniz,—Distributed photovoltaic generation and energy storage systems: A review, Renewable Sustainable Energy, Rev., vol. 14, no. 1, pp. 506–511, 2010.
- [3]. M. Bragard, N. Soltan, S. Thomas, and R. W. De Doncker, —The balance of renewable sources and user demands in grids: Power electronics for modular battery energy storage systems, I IEEE Trans. Power Electron., vol. 25, no. 12, pp. 3049–3056, Dec. 2010.
- [4]. Muhammad H. Rashid, —Power electronics circuits, devices and applications Pearson education, 3rd edition, 2004.
- [5]. Lewicki, Z. Krzeminski, and H. Abu-Rub, —Spacevector pulse width modulation for three-level npc converter with the neutral point voltage control, I IEEE Trans. Ind. Electron., vol. 58, no. 11, pp. 5076–5086, Nov., 2011.
- [6]. M. Miyatake, M. Veerachary, F. Toriumi, N. Fujii, and H. Ko, “Maximum power point tracking of multiple photovoltaic arrays: A PSO approach,” IEEE Trans. Aerosp. Electron. Syst., vol. 47, no. 1, pp. 367–380, Jan. 2011.
- [7]. J. T. Stauth, M. D. Seeman, and K. Kesarwani, “Resonant switched capacitor converters for sub-module distributed photovoltaic power management,” IEEE Trans. Power Electron., vol. 28, no. 3, pp. 1189–1198, Mar. 2013.
- [8]. T. Shimizu, M. Hirakata, T. Kamezawa, and H. Watanabe, “Generation control circuit for photovoltaic modules,” IEEE Trans. Power Electron., vol. 16, no. 3, pp. 293–300, May 2001.
- [9]. H. J. Bergveld et al., “Module-level dc/dc conversion for photovoltaic systems: The delta-conversion concept,” IEEE Trans. Power Electron., vol. 28, no. 4, pp. 2005–2013, Apr. 2013.
- [10]. P. S. Shenoy, K. A. Kim, B. B. Johnson, and P. T. Krein, “Differential power processing for increased energy production and reliability of photovoltaic systems,” IEEE Trans. Power Electron., vol. 28, no. 6, pp. 2968–2979, Jun. 2013.
- [11]. J. H. Wohlgemuth and S. R. Kurtz, “How can we make PV modules safer?” in Proc. 38th IEEE Photovoltaic Spec. Conf., 2012, pp. 3162–3165.
- [12]. W. Li and X. He, “Review of non-isolated high-step-up dc/dc converters in photovoltaic grid-connected applications,” IEEE Trans. Ind. Electron., vol. 58, no. 4, pp. 1239–1250, Apr. 2011.

- [13]. H. Wang and D. Zhang, “The stand-alone PV generation system with parallel battery charger,” in Proc. IEEE ICECE, Jun. 2010, pp. 4450–4453.

AUTHOUR'S DETAILS:



G.S.S.V. PRASAD received his B.Tech degree from Srinivasa Institute of Engineering and Technology, Amalapuram. At present he is pursuing M.Tech in Gonna Institute of Information Technology & Sciences, Aganampudi, Visakhapatnam. His area of Interest is Power Electronics.



P.LAVANYA received her B.E degree from Sanketika Vidya Parishad, P.M.Palem, Visakhapatnam and his M.Tech from Dadi Institute of Engineering & Technology, Anakapalli. At Present she is working as Assistant Professor in Gonna Institute

of Information Technology & Science, Aganampudi, Visakhapatnam.